

## 5. VOLCANIC ASH AND PUMICE AT SHATSKY RISE: SOURCES, MECHANISMS OF TRANSPORT, AND BEARING ON ATMOSPHERIC CIRCULATION<sup>1</sup>

James H. Natland<sup>2</sup>

### ABSTRACT

Air-fall volcanic ash and pumice were recovered from 22 intervals in upper Miocene-Pleistocene nannofossil oozes cored in Hole 810C on Shatsky Rise, northwest Pacific. Shatsky Rise is near the eastern limit of ash falls produced by explosive volcanism in arc systems in northern Japan and the Kuriles, more than 1600 km away. Electron probe analyses establish that the ash beds and pumice pebbles are andesitic to rhyolitic in composition, and belong to both tholeiitic and high-alumina lineages similar to tephra from Japanese volcanoes. High-speed winds in the polar-front and subtropical jets are evidently what propelled the ash for such a distance. The pumice arrived by flotation, driven from the same directions by winds, waves, and currents. It is not ice-rafted debris from the north. One thick pumice bed probably was deposited when a large pumice mat passed over Shatsky Rise.

Far more abundant ash occurs in sediments cored at DSDP Sites 578 through 580, about 500 km west of Shatsky Rise. Most of the ash and pumice at Shatsky Rise can be correlated with specific ash beds at 1, 2, or all 3 of these sites by interpolating to precisely determined magnetic reversal sequences in the cores. Most of the correlations are to thick ash layers ( $5.7 \pm 3.0$  cm) at one or more sites. These must represent extremely large eruptions that spread ash over very wide areas. Whereas several of the thicker correlative ashes fell from elongate east-trending plumes directed from central Japan, the majority of them—dating from about 2 Ma—came from the North Honshu and Kurile arc systems to the northwest. This direction probably was in response to both long-term and seasonal fluctuations in the location and velocity of the polar-front jet, and to more vigorous winter storm fronts originating over glaciated Siberia.

“... one is encouraged to believe that the accumulation of ash deposits occurred in the past at a rate adequate enough to provide data on the general circulation of the atmosphere.”

—Gordon Eaton (1963)

### INTRODUCTION

A surprising bonus for the igneous petrologist participating on Ocean Drilling Program Engineering Leg 132 was the recovery of 12 air-fall volcanic-ash beds, 1 pumice bed, and 9 pumice fragments in the upper 70 m of Miocene and younger carbonate ooze piston cored in Hole 810C on Shatsky Rise (Table 1). Most of the ash beds are only 1–2 cm thick, but one of them is 8 cm thick and the pumice bed is 14 cm thick (Fig. 1). An X-ray-fluorescence chemical analysis obtained on board established that the thick pumice bed is a siliceous rhyolite of a type usually derived from island-arc environments (Shipboard Scientific Party, 1991). Since the nearest arc complex is Japan, more than 1600 km away, the two thickest beds must represent enormous explosive volcanic eruptions for so much ash and pumice to have traveled such a distance. Shatsky Rise itself is a Mesozoic igneous feature (e.g., Nakanishi et al., 1989) thickly capped with Cretaceous and younger marine pelagic sediments (e.g., Larson, Moberly, et al., 1975). Thus it is not a modern local source of tephra, and distant arcs must be the source of all the ash layers and the pumice.

A great many more ash beds were recovered by piston coring in Miocene and younger sediments at Sites 578 through 580 during Leg 86. The three sites form a north-south transect about 500 km west of Shatsky Rise. The ash beds were annotated on the barrel sheets and briefly described in the site reports of the Leg 86 *Initial Reports* volume (Heath, Burckle, et al., 1985). On the Japan margin, literally hundreds of ash beds were cored during DSDP Legs 56, 57, and 87 (summarized in Fujioka, 1986). The general distribution of ash, then, is one of increasing frequency of occurrence westward, pointing

generally to sources in Japan, and possibly the Kurile Islands and Kamchatka, with Shatsky Rise being near the eastern limit of deposition of ash layers sufficiently thick to survive bioturbation in pelagic sediments (Fig. 2).

The generally wide distribution of Pleistocene-Holocene ash east of Japan was first noted from piston cores (Ninkovich et al., 1966; Horn et al., 1969; Hays and Ninkovich, 1970). Ninkovich and Donn (1976) cited both climatic and volcanological factors for the dispersal of Pleistocene-Holocene ash east of Japan. The drilling results provide a means of extending the record of ash deposition on the seafloor in the northwestern Pacific further into the past. The occurrence of ash at Shatsky Rise suggests that potentially correlative ash beds might be encountered at drill sites anywhere between there and the northwestern Pacific trenches. The high-resolution bio- and magnetostratigraphy possible on sediments obtained by advanced hydraulic piston coring provides the means to establish such correlations.

This paper first provides descriptions and compositions of ash and pumice at Shatsky Rise, then summarizes the results of a companion study (Natland and Dieu, in prep.) on the frequency and distribution of ash in Holes 579 and 580 based on a new examination of the cores and integration with magnetostratigraphy (Bleil, 1985). Using the same procedures, I then establish that precise correlations can be made between individual ash layers at those sites and all but four of the ash layers and pumice fragments recovered in Hole 810C, based on the combined biostratigraphic and magnetostratigraphic summary of Premoli Silva et al. (this volume). The results imply that ash propagation (and pumice flotation) to Shatsky Rise has persistently been from the west and west-northwest—that is, the Japanese and Kurile arcs—since the Miocene.

### SETTING AND SUMMARY OF CORING RESULTS

Site 810 is located in the central part of Shatsky Rise (Fig. 3), which is an oceanic plateau considered to have formed by hot-spot volcanism along the migrating trace of the Pacific-Farallon-Izanagi triple junction (Nakanishi et al., 1989). The age and composition of volcanic basement, however, are uncertain because it is buried by a thick sequence of Mesozoic cherts and chalks that have not been

<sup>1</sup> Natland, J.H., Storms, M.A., et al., 1993. *Proc. ODP, Sci. Results*, 132: College Station, TX (Ocean Drilling Program).

<sup>2</sup> Rosenstiel School of Marine and Atmospheric Science, University of Miami, Miami, FL 33149, U.S.A.

**Table 1. Ash and pumice occurrences at Hole 810C with correlations to Sites 578 through 580.**

Hole 810C Core, section, interval (cm)	Type	Thickness (cm)	Depth (mbsf)	Age (Ma)	Correlations								
					(1)			(2)			(3)		
					Site	Age (Ma)	Thickness (cm)	Site	Age (Ma)	Thickness (cm)	Site	Age (Ma)	Thickness (cm)
1 2H-6, 13	*Pumice	—	10.04	0.40	579	0.39	5.0	578	0.41	2.5	580	0.41	Tr
2 3H-2, 8	*Pumice	—	13.84	0.56	—	—	—	—	—	—	—	—	—
3 3H-2, 117–118	Ash	1	14.57	0.59	578	0.58	6.0	579	0.60	2.0	580	0.60	Tr
4 3H-2, 138	*Pumice	—	14.78	0.60	—	—	—	—	—	—	—	—	—
5 3H-4, 148	*Pumice	—	17.88	0.75	578	0.75	2.0	579	0.75	(Pum.)	—	—	—
6 3H-6, 25	*Pumice	—	19.64	0.84	580	0.84	2.5	—	—	—	—	—	—
7 4H-1, 4–6	*Ash	2	21.44	0.97	579	0.98	5.0	580	0.99	2.0	—	—	—
8 4H-1, 8	*Pumice	—	21.48	0.97+	580	1.00	3.0	—	—	—	—	—	—
9 4H-1, 29	*Pumice	—	21.69	1.00	580	1.01	11.0	579	1.01	1.0	578	1.01	Tr
10 4H-2, 26–27	*Ash	1	23.16	1.14	580	1.15	4.0	579	1.14	2.5	578	1.16	1
11 4H-3, 134–135	*Ash	1	25.74	1.40	578	1.39	5.0	—	—	—	—	—	—
12 4H-4, 83–84	*Ash	1	26.72	1.49	580	1.51	7.0	—	—	—	—	—	—
13 4H-6, 98	*Pumice	—	29.88	1.81	580	1.80	7.0	579	1.80	2.0	—	—	—
14 4H-7, 57	*Pumice	—	30.97	1.92	580	1.92	2.5	—	—	—	—	—	—
15 5H-3, 47–48	*Ash	1	34.37	2.26	580	2.26	10.0	579	2.27	7.0	578	2.23	3.0
16 5H-4, 147–149	*Ash	2	36.87	2.40	579	2.38	8.0	578	2.39	4.0	580	2.39	0.5
17 5H-5, 64–65	*Ash	1	37.54	2.44	580	2.46	3.5	579	2.44	1.0	—	—	—
18 6H-1, 12–20	*Ash	8	40.52	2.54	580	2.53	3.0	579	2.54	2.5	—	—	—
19 6H-1, 43–44	*Ash	1	40.83	2.62	579	2.61	4.0	580	2.63	4.0	578	2.63	Tr
20 6H-6, 18–32	*Pumice bed	14	48.08	2.99	578	2.96	7.0	579	2.99	3.0	—	—	—
21 8H-2, 90–91	*Ash	1	62.30	3.83	—	—	—	—	—	—	—	—	—
22 9H-1, 54–55	*Ash	1	69.44	4.44	578	4.46	13.0	—	—	—	—	—	—

\*Electron probe glass analyses given in Table 2.

penetrated by drilling (Larson, Moberly et al., 1975). The cherts and chalks in turn are capped by Paleogene-Neogene carbonate oozes.

Drilling the cherts and chalks with the experimental diamond coring system was one of the objectives of Engineering Leg 132. The choice of site was dictated by the requirement to have precisely 100–120 m of the younger ooze overlying the chert-chalk sequence, and for the chert to be as shallow as possible (Storms and Natland, 1991). The site was approached from the southwest, while the under-way watch monitored seismic profiler records showing steady shoaling of the reflective cherts, and first thickening and then thinning of the overlying pelagic cap (Fig. 4). Before the pelagic cap thinned to the required 100–120 m of carbonate ooze, however, we crossed a gully evidently produced by current erosion. Consequently, the beacon was dropped atop a flat elevation between two such gullies, but with an appropriately thin capping of ooze above the chert-chalk sequence. The capping is thinner than across the gully to the south, largely because—as coring later showed—the Paleogene–lower Neogene section was extremely reduced by erosion. The entire Oligocene to lower Miocene interval is missing.

Despite the proximity of gullies, we obtained a nearly complete section of upper Miocene to Pleistocene sediments, deposited at an almost uniform rate of 15 m/m.y. (Premoli Silva et al., this volume). There are no missing magnetic transitions in this interval, and only two small disconformities are inferred in the Pleistocene. The 12 occurrences of ash, the thick pumice bed, and the 9 pumice dropstones are indicated together with the magnetic stratigraphy in Figure 5.

A few ash beds and pumice fragments were recovered previously from Shatsky Rise at DSDP Sites 47 and 50 (Fischer, Heezen, et al., 1971), 308 (Larson, Moberly, et al., 1975), and 577 (Heath, Burckle, et al., 1985). At the first three sites, many ash beds were probably destroyed by sediment deformation during rotary coring. Others were missed because of incomplete recovery and discontinuous coring. Site 577 was piston cored, yet only 3 thin ash beds and 1 ashy interval were recovered in Pliocene sediments. Sites 577 and 810 are only 11.7 km apart, and are at nearly the same depths. Similar Neogene sections were recovered. Why fewer ash beds were found at Site 577, and why in particular the thickest ash bed and the pumice bed were not recovered there, are puzzling. However, sediments younger than the Gilbert magnetochron are 18 m thinner at Site 577 than at Site 810 (Sager et al., this volume, fig. 4). The section from Site 577 thus may

have more numerous small erosional unconformities than from Site 810, therefore fewer ash layers.

Most ash beds at Site 810 are only 1–2 cm thick. They are very light gray or light brownish gray (the “white” ash of Horn et al., 1969). Beds thinner than this evidently are dispersed beyond visual recognition by burrowing organisms, but may show up as spikes in glass content in smear slides (Shipboard Scientific Party, 1991). The beds are poorly consolidated and gritty, and some are burrowed. The thick ash bed and the pumice bed are among the oldest recovered, being 18th and 20th with depth in the sequence of 22 ash and pumice occurrences. Individual fragments in the pumice bed are 0.5–1.0 cm in diameter.

The nine pumice fragments were recovered from upper Pliocene and Pleistocene sediments. The first encountered, at 10.04 meters below the seafloor (mbsf), is 4.5 cm in longest diameter and is distinctly rounded. The remainder are each less than 1 cm in diameter and also rounded. No lithic clasts were encountered. Site 810 is below the latitude of even rare ice-rafted debris—mainly volcanic and sedimentary rock, not pumice—found in piston cores, dredge hauls, or drill sites in the northwest Pacific (Fig. 2; Kuno et al., 1956; Conolly and Ewing, 1970; Krissek et al., 1985; Dieu, 1990). The pumice here evidently was not ice-rafted from the north, but floated in under prevailing winds, waves, and currents from the direction of Japan (Fig. 2).

## PETROGRAPHIC CONTRASTS BETWEEN ASH AND PUMICE

Examination of polished mounts in reflected light shows that particles in the ash beds are predominantly angular and elongate shards of bubble-wall volcanic glass (Fig. 6A) with small amounts of mineral grains, chiefly broken plagioclase with lesser pyroxenes, amphiboles, and oxides. Glass fragments are 20–300  $\mu\text{m}$  in length. Rhyolitic glass fragments are colorless in transmitted light, and andesite glass is tinted faintly brown. Many of the glass shards are long and straight, indicating that bubbles were highly stretched before fragmentation occurred. Some preserve wishbone-like joins where bubble-walls met. Most shards are very narrow, only 10–15  $\mu\text{m}$ , and thus have aspect ratios of 2–20. Most bubbles thus were large and separated by thin walls of glass before disruption. Only a very few glass shards completely

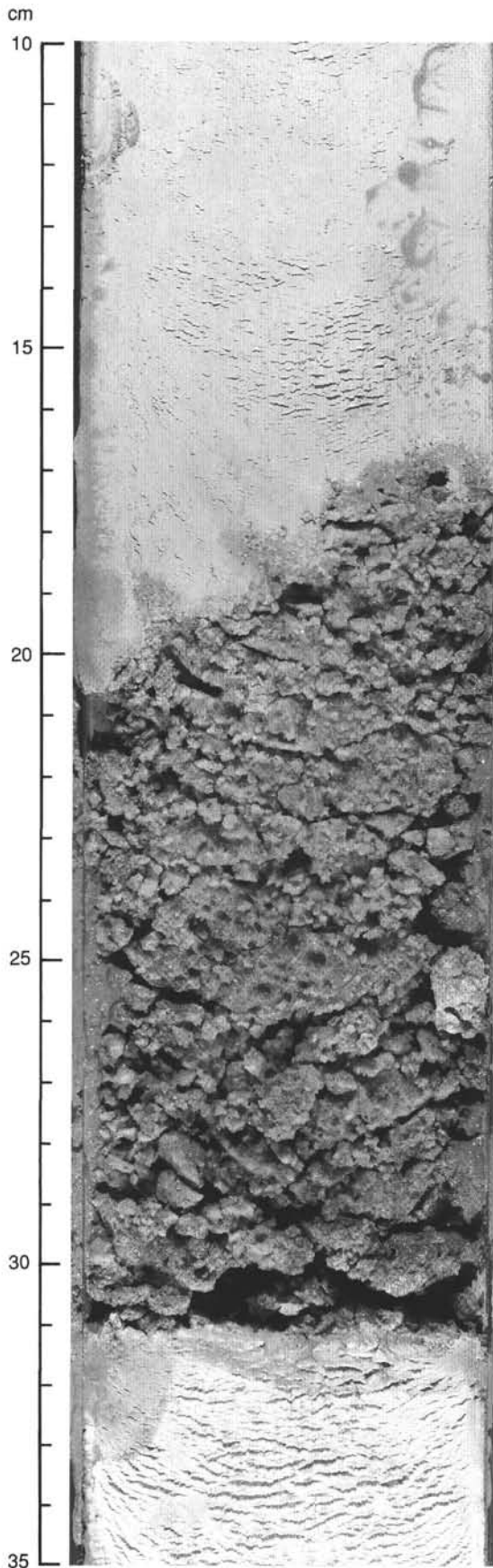


Figure 1. Coarse pumice bed, 14 cm thick, with irregular top, in Core 132-810-6H-6. The age of the bed is 2.99 Ma, based on interpolation to the magnetic reversal sequence in the cores (Table 1).

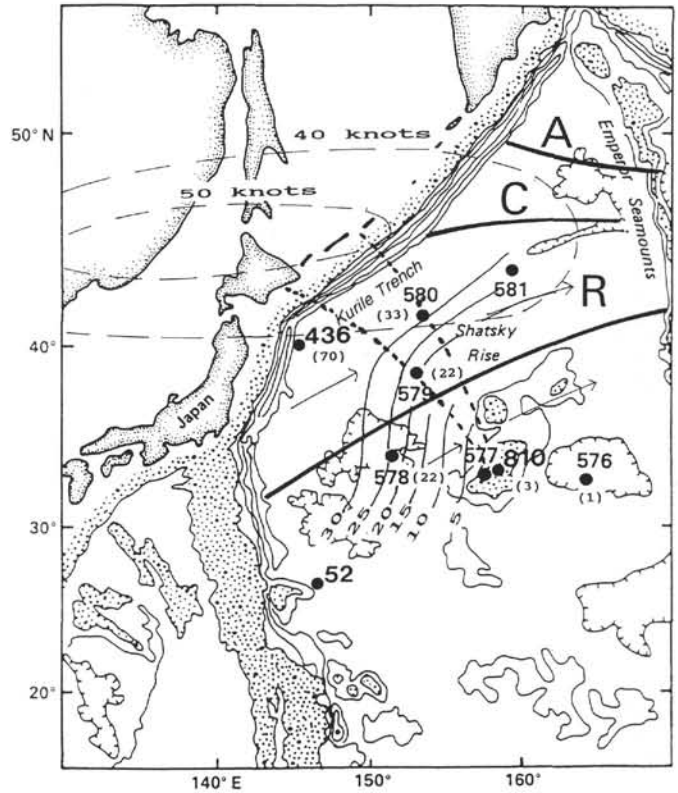


Figure 2. Distribution of volcanic ash at DSDP and ODP sites (numbered dots) east of Japan. Numbers in parentheses give average number of ash beds at each site per million years over the past 3 m.y. Contours are also in number of ash beds per million years over the past 3 m.y. Bold lines delimit relative abundance of ice-rafted material in Pleistocene sediments (Conolly and Ewing, 1970; Krissek et al., 1985): A = abundant; C = common; R = rare. Arrows give the general direction of surface currents, related to the Kuroshio current, east of Japan. The position of the subtropical jet in July 1950 is given by dashed contours labeled with average wind speed in knots (nmi/hr) (Reiter, 1963). Site 810 ashes, correlated with those from northerly Sites 579 and 580, originated along the sector of Hokkaido and the Kurile Islands between the two bold dashed curves. These are great-circle trajectories through Sites 579 and 580 to Site 810, along azimuths  $120^\circ$  and  $145^\circ$ , respectively.

enclose bubbles, and in those cases, the bubbles are  $<5\mu\text{m}$  in diameter. The typical sizes and shapes of the glass shards suggest that the volume of bubbles may have exceeded 80% when fragmentation occurred. Mineral fragments are typically 20–50  $\mu\text{m}$ , but in one rhyolitic ash a euhedral plagioclase enclosing smaller grains of magnetite and amphibole is still preserved. It is  $1520 \times 930 \mu\text{m}$ .

A pumice fragment from the large pumice bed was examined in reflected light (Fig. 6B). The proportions and sizes of bubbles were measured using a Leica Quantimet 500 image analyser. One  $0.44\text{-cm}^2$  area contains 44.6% bubbles with an average maximum diameter of 28.6  $\mu\text{m}$  and an average minimum diameter of 15.5  $\mu\text{m}$ .

The average aspect ratio is 2.03. The maximum aspect ratio measured was 6.5, and the largest bubble diameter was 445  $\mu\text{m}$ . Glass-wall diameters are from 10 to 20  $\mu\text{m}$ , or about one-third to two-thirds of the average maximum bubble diameter. Smaller areas ( $0.2\text{--}0.3 \text{ cm}^2$ ) measured on other pumice fragments from the same sample have similar bubble sizes and aspect ratios but are variably vesicular, containing as little as 28% and as much as 56% bubbles. The several mounted fragments together contain a few phenocrysts of plagioclase and amphibole between 0.3 and 0.7 mm in length.

The ash material just before fragmentation thus was more vesicular and contained larger and more elongate bubbles than the pumice.

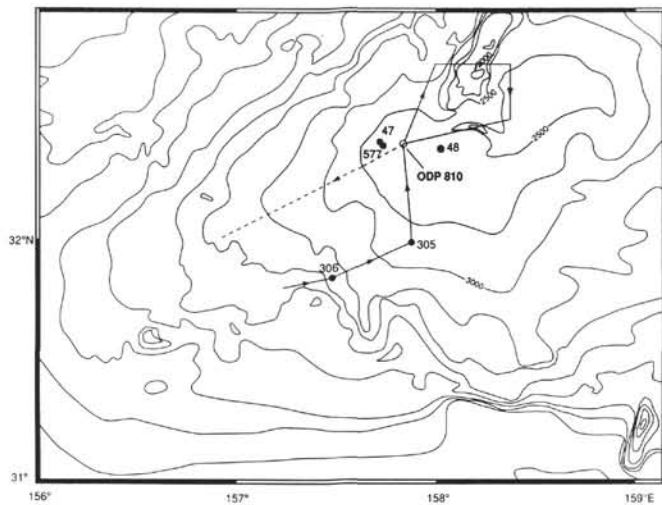


Figure 3. Bathymetry of a part of Shatsky Rise (250-m contours) showing the locations of DSDP sites and ODP Site 810. The incoming seismic line linking DSDP Sites 305 and 306 with Site 810 (Figure 4) is shown as a solid line. The track of a post-site seismic survey is shown by a dashed line. Other DSDP sites are shown.

The differences may have resulted from projection higher into the atmosphere, which facilitated expansion of gases. The elongation of the bubbles may have resulted from ablation and stretching of the molten and vesicular material before it fragmented into ash.

### COMPOSITIONS OF ASH AND PUMICE

Compositions of siliceous volcanic glass from five ash beds and two pumices cored in Hole 810C on Shatsky Rise are listed in Table 2. Analyses were obtained using a Camebax microbeam electron probe at Scripps Institution of Oceanography. Most analyses represent averages of several spots on large shards or pumice fragments, or of several compositionally identical glass shards in individual samples (given as  $n$  in Table 2). One ash bed (Sample 810C-5H-5, 64–65 cm) consists predominantly of rhyolitic glass, with rare fragments of differing composition. The latter are represented by single analyses ( $n = 1$ ) in Table 2.

The standardization was modified from procedures for basalt glasses described by Natland et al. (1983). That is, USNM basalt glass standard VG-2 was run regularly as an unknown, and most oxides were normalized to it. Exceptions were  $K_2O$  in all glasses, and  $SiO_2$  and  $Al_2O_3$  in rhyolites, which were calibrated to USNM microcline. A serious problem was the volatility of  $Na_2O$  under the probe beam, especially in rhyolites. This was overcome by defocusing the probe beam to at least 20  $\mu m$ , and rastering the beam by hand over 100–200  $\mu m^2$  areas of glass shards that were generally quite irregularly shaped. This procedure was devised by trial and error. Results were deemed acceptable only when consistent  $Na_2O$  values were obtained (the  $2\sigma$  variation ranged from 0.14% to 0.38% for several multipoint analyses), and totals exceeded 94%. Differences between totals and 100% are presumably due to the presence of combined water ( $H_2O^+$ ).

Ash Sample 132-810C-3H-2, 117–118 cm, consists of two similar types of andesite. Sample 132-810C-5H-5, 64–65 cm, consists predominantly of rhyolite glass shards, but also of a small percentage of diverse glass fragments ranging in composition from andesite to rhyodacite. The remaining samples contain exclusively rhyolite glass. In four samples, including a pumice fragment from the thick pumice bed (132-810C-6H-6, 18–32 cm), the rhyolite is especially siliceous (76.5%–78.7%  $SiO_2$  based on totals normalized to 100% in Table 2). One pebble from the pumice bed is significantly more siliceous (78.2%  $SiO_2$ ) than the shipboard bulk XRF analysis (71.8%  $SiO_2$ ; Shipboard

Scientific Party, 1991), suggesting that the pumice is not homogeneous. CIPW norms of the rhyolites (Table 2) indicate that they are metaluminous to mildly peraluminous (maximum 1.04% normative corundum). The samples contain fragments of quartz, plagioclase, pyroxenes, amphiboles, magnetite, and ilmenite. Aluminous minerals such as muscovite, cordierite, garnet, and aluminosilicates are absent. The amounts of quartz and corundum in the norms of rhyolites can be enhanced if some  $Na_2O$  was lost during the probe analysis, but normative differences in Table 2 are genuine, since  $Na_2O$  loss was minimized, as described above, and all samples were analyzed in the same manner.

The glasses correspond to intermediate and siliceous portions of the tholeiitic and high-alumina trends of Japan (Fig. 7), long ago established by Kuno (1965). Rhyolites at the high- $SiO_2$  ends of the two trends differ in total alkalis, chiefly because of differences in  $K_2O$  contents. Three rhyolites of the high-alumina trend (group 1 in Figure 7) have  $K_2O$  contents of >3.8%; those falling along the tholeiitic trend (group 2) have  $K_2O$  contents of <2%. In all respects described here, the glasses are indistinguishable from electron probe compositions obtained on glass from ash recovered at DSDP sites near Japan, which was derived from the Tohoku and North Honshu arcs (Fujioka, 1986).

Analyses of plagioclases, pyroxenes, amphiboles, and oxide minerals were also obtained by electron probe. Some of the pyroxenes are more magnesian, and the plagioclases more calcic, than could have crystallized from rhyolitic liquids. The mineral compositions thus augment the picture of sample heterogeneity indicated by the glass analyses, and suggest that magma mixing, incorporation of restite, or both, were involved in the petrogenesis of the ash and pumice that reached Shatsky Rise.

### SUMMARY OF OBSERVATIONS ON ASH IN CORES FROM SITES 578 THROUGH 580

The possibility that ash beds and pumice at Site 810 might correlate with the ash stratigraphy at Sites 578 through 580, cored west of Shatsky Rise during Leg 86, prompted a new examination of the cores from those sites (Natland and Dieu, in prep.). There are 266 ash beds in cores from the three sites, ranging from discontinuous splotches distorted by burrowing organisms to well-defined beds up to 20 cm thick. The beds are pale gray or pale brownish gray siliceous volcanic glass, with minor amounts of fragmental pyroxenes, amphiboles, feldspars, and oxide minerals. Ash occurrences date from the Miocene, but are most abundant in upper Pliocene to Holocene sediments.

A precise chronostratigraphy exists for Sites 578 through 580, based on locations of magnetic reversals in the cores (Bleil, 1985) and the timing of those reversals (Berggren et al., 1985). Ages of ash beds were estimated by linear interpolation of positions of ash beds relative to the magnetic reversals in the cores. Linear interpolation assumes that sedimentation rates were constant within each chron and subchron (c.f. Heath et al., 1985), and that sediments were not vertically distorted by the coring process. The latter is the case for most of the cores, but deformation is noticeable in the very topmost sediments (0–15 m below the seafloor) recovered at each site.

Obviously, ages can be assigned with greatest confidence where magnetic reversals are closely spaced. The greatest uncertainty is in the mid-sections of intervals spanning long chrons or subchrons where more than two cores (9.5 m apiece) were taken between reversals (i.e., the Brunhes, from 0 to 0.7 Ma, and a part of the Matuyama, from 0.98 to 1.66 Ma). In such cases, the maximum accumulated depth error is probably no more than 1 m, combining uncertainty in the residual (not completely compensated) heave of the vessel during coring operations, and imprecision in the length of pipe joints (about 0.2 m; Shipboard Scientific Party, 1979). This represents about 0.04 m.y. in an age estimate, based on sedimentation rates at these sites.

Cumulative ash frequency and thickness curves can be compared for all three sites (and for Site 810) for the past 3.2 m.y. The comparisons show that there was a sharp increase in ash deposition

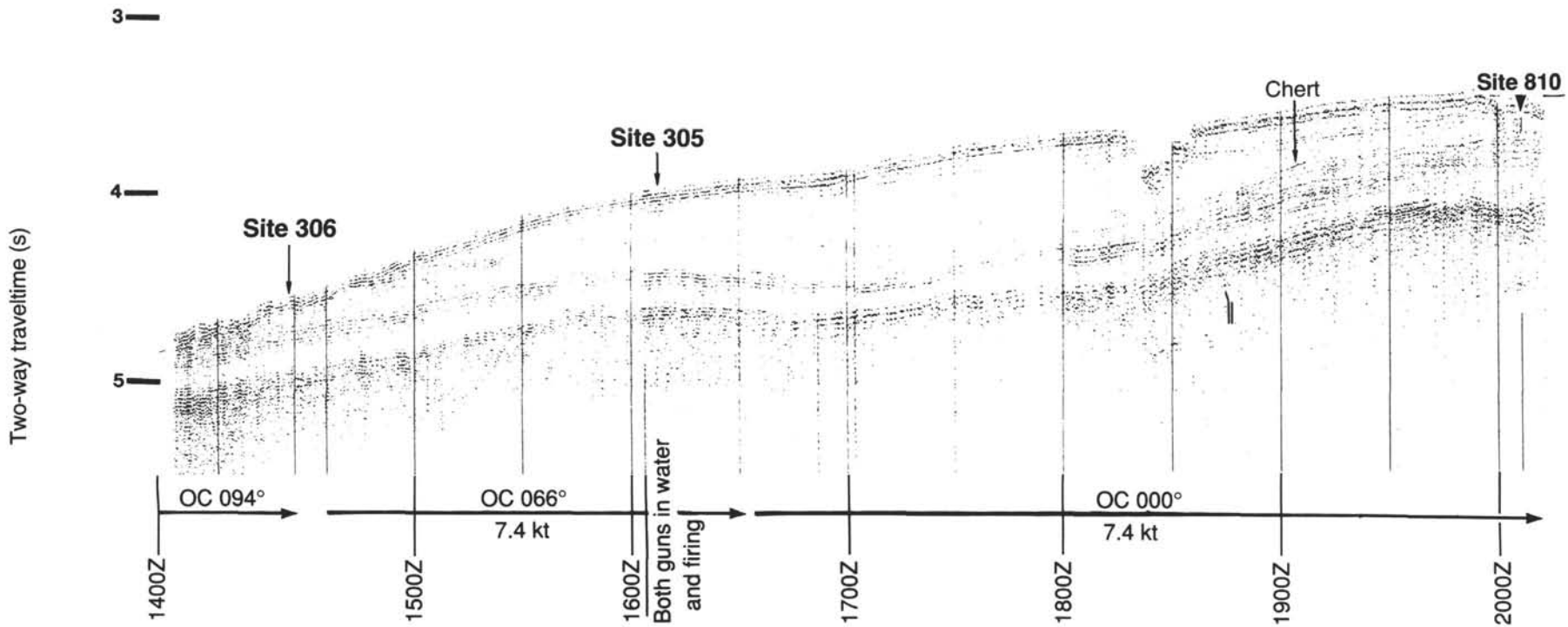


Figure 4. *JOIDES Resolution* seismic profiler record obtained during the approach to Site 810 on Shatsky Rise. The arrow indicates the principal seismic reflector (chert zone) traced beneath the sediment cap.

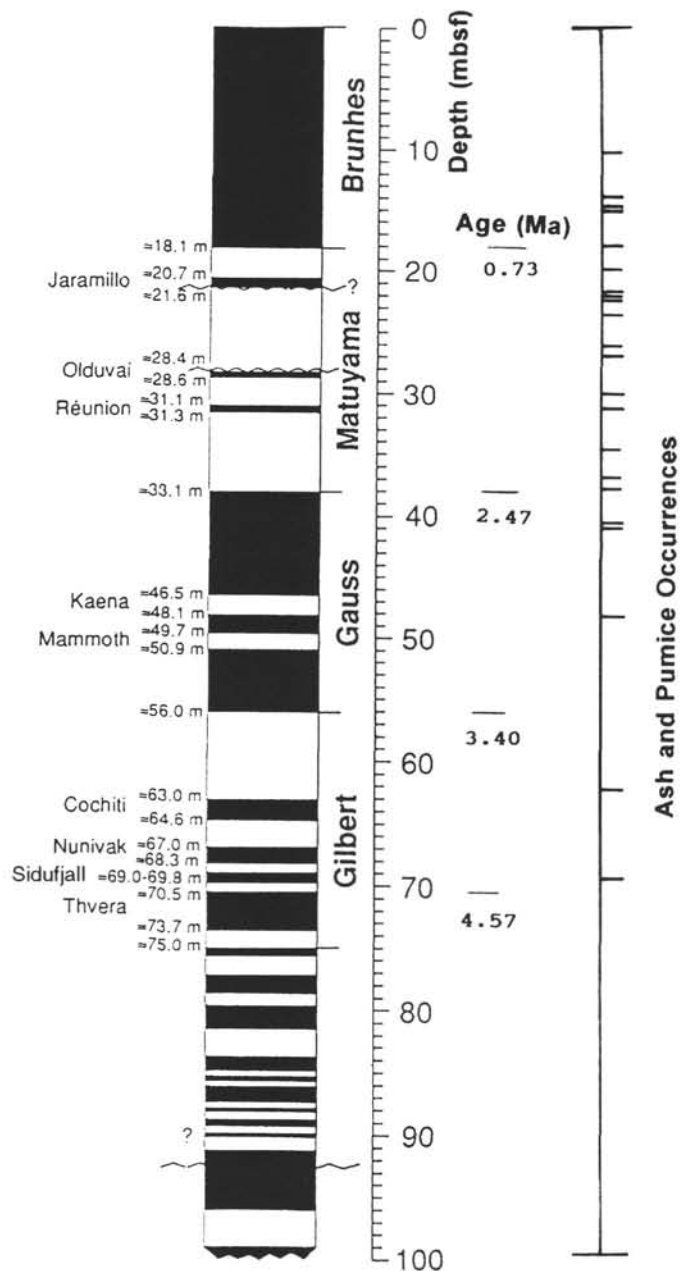


Figure 5. Occurrences of ash and pumice vs. depth in Hole 810C, compared with magnetic reversal stratigraphy obtained on board *JOIDES Resolution*, from Premoli Silva et al. (this volume). Ages are from Berggren et al. (1985).

toward the south, beginning about 3 Ma. Subsequently, periods of similarity in north-south ash-accumulation rates alternated with periods of greater accumulation to the north. Most surprisingly, a marked episodicity in ash frequency corresponded to 100,000-yr cycles in orbital parameters influencing Earth's climate, strongly apparent since 1.4 Ma (Natland and Dieu, in prep.). A longer period accentuation also exists, with broad peaks in ash frequency and accumulation from about 2.5–2.1 Ma, 1.4–0.6 Ma, and the past 0.2 m.y.

The Japanese and Kurile arc systems lie beneath the polar-front and subtropical jet streams. Natland and Dieu (in prep.) suggest that all of these variations in ash distribution reflect changes in the positions, velocities, and perhaps widths of these jets over the north-west Pacific since late Miocene time. Although jet-stream dispersal of volcanic ash projected high into the atmosphere is no surprise, what is most useful about the results is that ash stratigraphy can provide

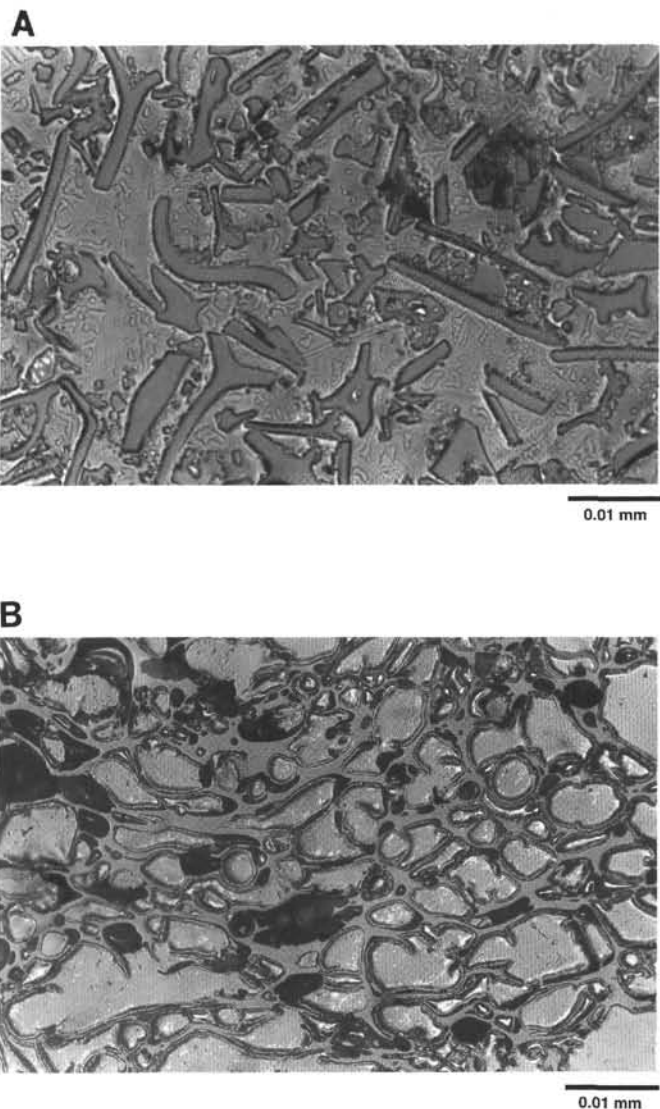


Figure 6. Photomicrographs in reflected light of angular rhyolitic bubble-wall shards in ash Sample 132-810C-5H-5, 64–65 cm (A), and rhyolite pumice Sample 132-810C-6H-6, 18–32 cm (B). Both field widths are 0.7 mm.

information about the location and intensity of jets during the entire period of global climatic harshening since the Pliocene. Moreover, dispersed ash almost exclusively reflects wind speed, with no other climatic factors (i.e., aridity) involved. Finally, the jets, in which winds can reach 160–250 km/hr (Reiter, 1963), are most likely the mechanism of occasional dispersal of ash all the way to Shatsky Rise.

Two comparisons provide some indication of both the dimensions of eruptions from volcanoes in the Japanese and Kurile arc systems, and the effectiveness of high-speed atmospheric jets in dispersing their ash. The 18 May 1980 eruption of Mount St. Helens (at 47°N) produced a blanket of air-fall ejecta that had a maximum thickness of 4 cm about 300 km east-northeast of the volcano (Sarna-Wojcicki et al., 1981). At a distance of 420 km, the ash was no more than 1 cm thick. The 4-cm isopach surrounds a local high (the “distal thickness maximum” of Sarna-Wojcicki et al., 1981) in the ash thickness. Between there and Mount St. Helens, the ash thins to less than 2 cm, then thickens again in the immediate vicinity of the volcano. The cause of this is uncertain, but Sarna-Wojcicki et al. cite J.G. Moore (written commun., 1980), who suggested that differential fallout of ash erupted above, into, and below the high-velocity wind layer 10–13 km above the volcano to account for ash thicknesses at the local high, farther to the east, and near the volcano, respectively. Several later

Table 2. Electron probe analyses of ash and pumice, Hole 810C, Shatsky Rise.

	Core-section-glass group													
	3H-2A	3H-2B	3H-6	4H-1A	4H-1B	4H-3	5H-3	5H-5A	5H-5B	5H-5C	5H-5D	5H-5E	5H-5F	6H-6
<i>n</i>	5	1	5	1	5	4	5	2	1	1	1	1	5	4
SiO <sub>2</sub>	56.63	57.71	72.00	77.99	78.69	76.51	76.99	56.23	60.31	62.52	64.71	66.56	74.00	78.16
TiO <sub>2</sub>	1.18	1.03	0.49	0.32	0.33	0.08	0.10	1.12	1.30	1.11	0.31	0.62	0.30	0.21
Al <sub>2</sub> O <sub>3</sub>	18.46	19.05	14.42	11.86	12.02	13.15	12.99	14.37	16.00	13.41	17.24	14.37	14.04	12.46
FeO*	7.30	6.36	3.40	1.85	1.87	1.24	1.22	14.11	8.07	8.89	3.70	5.65	1.38	1.35
MnO	0.19	0.16	0.17	0.06	0.06	0.02	0.06	0.17	0.16	0.17	0.05	0.23	0.10	0.10
MgO	2.89	2.06	0.68	0.24	0.25	0.06	0.08	3.04	1.76	2.67	1.96	2.68	0.70	0.20
CaO	6.75	7.20	3.10	1.54	1.56	0.71	0.86	6.09	5.78	5.94	5.31	3.23	1.07	1.46
Na <sub>2</sub> O	3.84	3.99	4.78	4.36	4.31	4.26	3.83	2.81	3.76	3.51	4.50	4.03	4.34	4.49
K <sub>2</sub> O	2.23	1.92	0.87	1.85	0.88	3.96	3.84	1.87	2.61	1.51	2.03	2.41	4.04	1.53
P <sub>2</sub> O <sub>5</sub>	0.53	0.47	0.09	0.03	0.03	0.01	0.03	0.19	0.25	0.27	0.19	0.22	0.03	0.04
Σ	95.79	94.59	94.97	95.83	94.62	95.15	95.89	94.43	97.88	97.20	95.74	99.53	94.11	95.79
Mg#	0.451	0.402	0.293	0.212	0.217	0.091	0.120	0.309	0.311	0.384	0.523	0.496	0.513	0.235
	CIPW norms													
Q	5.15	7.39	31.41	41.48	45.52	34.17	37.31	8.80	11.38	17.64	15.66	20.33	29.23	42.00
C	0.00	0.00	0.19	0.12	0.28	0.59	1.04	0.00	0.00	0.00	0.00	0.00	0.65	0.86
Or	13.16	11.33	5.13	10.92	5.19	23.37	22.66	11.04	15.40	8.91	11.98	14.22	23.84	9.03
Ab	32.47	33.73	41.41	36.02	36.44	36.02	32.38	23.76	31.79	29.68	38.05	34.07	36.69	37.96
An	26.53	28.38	14.78	7.44	7.54	3.45	4.07	21.06	19.06	16.36	20.83	13.99	5.11	6.96
Wo	1.45	1.77	0.00	0.00	0.00	0.00	0.00	3.29	3.32	4.72	1.77	0.24	0.00	0.00
En	0.67	0.74	0.00	0.00	0.00	0.00	0.00	1.01	1.11	1.84	0.88	0.12	0.00	0.00
Fs	0.77	1.04	0.00	0.00	0.00	0.00	0.00	2.41	2.31	2.95	0.86	0.12	0.00	0.00
En	6.77	4.60	1.93	0.68	0.70	0.18	0.28	6.77	2.48	5.03	4.06	6.73	1.88	0.64
Fs	7.83	6.45	4.10	2.14	2.16	1.67	1.60	16.12	7.21	8.07	3.97	7.02	1.51	1.60
Mt	1.72	1.50	0.80	0.43	0.43	0.29	0.29	3.33	1.89	2.10	0.87	1.33	0.32	0.32
Il	2.24	1.96	0.93	0.61	0.63	0.15	0.19	2.13	2.47	2.10	0.59	1.18	0.57	0.40
Ap	1.22	1.09	0.21	0.07	0.07	0.02	0.07	0.44	0.58	0.62	0.44	0.51	0.07	0.09

Note: Full sample identifications are given for samples with an asterisk (\*) in Table 1. This table gives cores, sections, and glass groups (alphabetically); *n* gives the number of spots or shards analyzed per sample. Analyses are listed normalized to 100%, based on the summation Σ as reported. Mg#’s and CIPW norms are calculated assuming  $Fe^{2+}/(Fe^{2+} + Fe^{3+}) = 0.86$ .

eruptions did not produce columns that reached this height, their ash was distributed by lower atmosphere winds in other directions, and they have no distal thickness maxima (Sarna-Wojcicki et al., 1981).

Similarly, the 1-cm isopach of the Roseau ash, produced by a Pleistocene eruption of the Lesser Antilles volcano Dominica at 15.5°N, extends about 750 km east of the volcano (Carey and Sigurdsson, 1980). The most distant part of the 4-cm isopach is 470 km to the east-southeast. The maximum thickness, 8 cm, is 300 km from Dominica in the same direction, but three piston cores between this maximum and the island have 1.5, 3.5, and 4.0 cm thicknesses of the ash. This suggests the presence of a “distal thickness maximum” here as well.

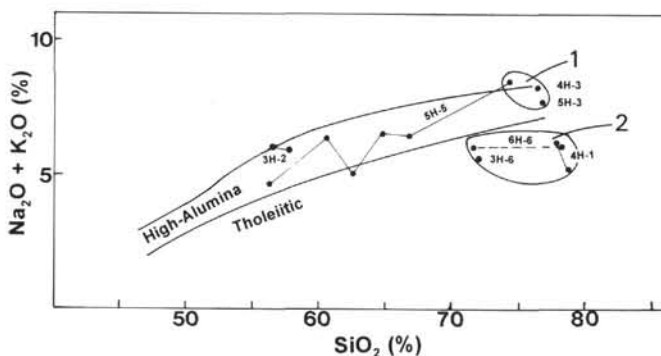


Figure 7. Total alkalis vs. SiO<sub>2</sub> for siliceous volcanic glass in pumice and ash from Hole 810C, Shatsky Rise. The bold lines delimit fields for tholeiitic and high-alumina series from Japan (Kuno, 1965). Thin solid lines link electron probe glass compositions from individual samples. The dashed line links a glass composition of a pebble from the thick pumice bed of Figure 1 with the corresponding bulk composition obtained by X-ray fluorescence aboard *JOIDES Resolution* (Shipboard Scientific Party, 1991). Groups 1 and 2 represent rhyolites of the high-alumina and tholeiitic trends, respectively, at Site 810.

At Sites 578 through 580, about 1000 km from Japan, 75 ash beds are  $\geq 4$  cm thick, or 28.6% of the total. These average 7.1 cm thick, with 10 ash beds being  $\geq 10$  cm thick. The 8-cm ash bed in Hole 810C, deposited when Shatsky Rise was more than 1900 km from Japan, is in this range of thicknesses. Obviously, these represent eruptions much larger than the May 1980 Mount St. Helens and Roseau eruptions. Indeed, such thicknesses at  $>1500$  km distance from sources suggest comparison to the great eruption at Toba, Sumatra, at 75 Ka, which produced an ash bed uniformly 8–10 cm thick at distances from 1000 to 2000 km from the volcano (Ninkovich et al., 1978). The total volume of pyroclastic material erupted at Toba was at least 2800 km<sup>3</sup>, of which 800 km<sup>3</sup> is estimated to be dispersed ash, as calculated from an isopach constructed from more than a dozen piston-core locations in the Indian Ocean widely distributed over nearly 4 million square kilometers (Rose and Chesner, 1987). This is the largest documented Quaternary marine ash layer (Ninkovich et al., 1978).

### CORRELATIONS BETWEEN SITES 810 AND 578 THROUGH 580

The isopachs for the Mount St. Helens and the Roseau ashes both show that Northern Hemisphere tropospheric winds may carry ash nearly directly east. This is the typical, but not exclusive, direction of jet streams. Divergences both to the north and south occur, particularly in response to seasonal weather patterns (Reiter, 1963). The Mount St. Helens and Roseau isopachs also have length:width aspect ratios of about 3:1 to 2:1, respectively. This suggests that for the north-west Pacific transect Sites 578 through 580 we may typically expect a number of correlations between two sites, 3°–5° apart, but far fewer correlations between all three sites, spanning 7.6° of latitude (835 km). On the other hand, each ash or pumice that reached Shatsky Rise could well have at least one correlative ash at the sites to the west.

The procedures for determining ages for the ash beds and pumice occurrences at Site 810 were the same as those used for Sites 578 through 580. Stratigraphic positions in cores were related to precisely located magnetic reversals determined using the shipboard cryogenic

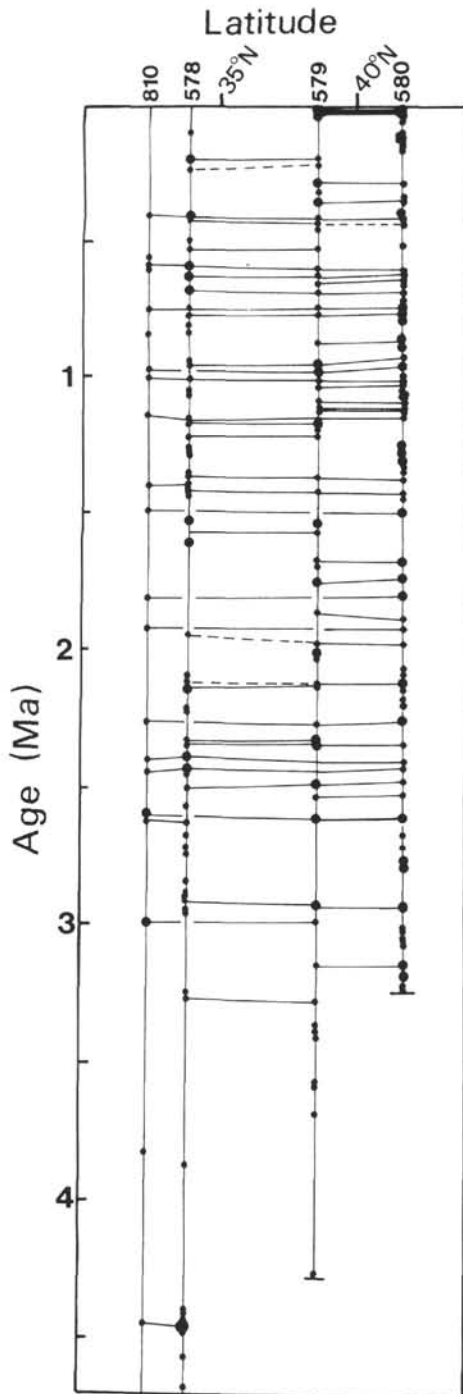


Figure 8. Ash and pumice occurrences at DSDP Sites 578 through 580 and ODP Site 810, compared according to ages estimated from magnetic reversal stratigraphy. Large dots are for ash beds  $\geq 4$  cm thick. Potential correlations (as defined in the text), linking occurrences that differ in age by  $<0.03$  Ma, are given by solid lines. Possible but less likely correlations are shown as dashed lines.

magnetometer (Shipboard Scientific Party, 1991). The reversal sequence was calibrated using nanofossil biostratigraphy by Premoli Silva (this volume) and is almost identical to that of Sager et al. (this volume), despite some difficulties with the shipboard magnetometer. Ages of the reversals, again, are those of Berggren et al. (1985). The estimated ages determined by interpolation of ash and magnetostratigraphic positions are given in Table 1.

Figure 8 gives all ash occurrences by age at Sites 578 through 580 and 810, with the most probable correlations between holes indicated by solid lines. Correlations are inferred only between adjacent holes. In several cases, there were virtually simultaneous ash falls at Sites 578 and 580, but not between these two sites at Site 579. In such cases, no correlations are drawn. A few possible, but not plausible, correlations (between trace thicknesses of ash at adjacent sites) are dashed.

Correlations are possible for all four holes back to 3.26 Ma, and for all but Site 580 to 4.26 Ma. Only Site 578 can be correlated to Site 810 beyond this. As noted above, age mismatches of 0.04 Ma correspond to about 1 m of sediment at Sites 578 through 580. Such mismatches in correlation are hardly possible between closely spaced magnetic reversals. All inferred correlations given in Figure 8 vary by  $<0.03$  Ma, and usually by  $<0.02$  Ma.

The correlations exist only in the sense implied by interpolated magnetostratigraphy, i.e., in time. Whether they represent exactly the same eruptions as opposed to, say, different ash layers deposited at almost exactly the same time cannot be said without geochemical comparisons. This is unlikely given that many of the two- and three-hole correlations in Figure 8 have no other events or perhaps only one event between them in any of the three holes; thus the average time between ash falls at given sites was fairly long. Each correlation would then have to represent two or more eruptions widely separated in space suddenly having occurred nearly simultaneously, and this having happened a very high percentage of the time out of a total number of events recorded.

Figure 8 therefore should be considered predictive, presenting correlations that can be tested by comparing compositions. For now, they can be considered *potential* correlations, with a strong likelihood of representing single eruptions.

The percentage of potential north-south correlations between the three transect holes is as follows. Of 239 ash beds in the 3 holes dating from 3.2 Ma to the present, there are 32 potential 2-hole correlations (=64 ash beds at two sites) and 16 potential 3-hole correlations (48 ash beds at 3 sites). If all of these correlations are correct, 175 explosive volcanic eruptions were recorded at the three sites. At Sites 578 and 579, 13 additional events date back to 4.48 Ma, none correlating, but one of which correlates with the deepest ash of Hole 810C. The yield of potential two-hole north-south correlations out of 188 events is therefore a maximum of 17.0%, and of potential three-hole correlations, 8.5%. The maximum total percentage of events with potential correlations is 25.5%.

Correlations to Hole 810C are given by site in Table 1, with interpolated ages and thicknesses. The three correlation columns give (1) a *primary* correlation to the thickest occurrence at one of the three sites; (2) a *secondary* correlation to a coeval thinner bed at another site, if one exists; and (3) a *tertiary* correlation to generally very thin coeval beds at the third site, if one exists.

Significantly, there is a very high yield of potential correlations between at least one of Sites 578 through 580 and Site 810 (19 of the 22 ash and pumice occurrences, or 86%). The yield of potential correlations between Site 810 and at least two sites to the west is also high, 59%. Even the percentage of potential correlations between Site 810 and all three sites to the west is 32%. Of two-hole and three-hole north-south correlations between Sites 578 and 580, 23% are also recorded at Site 810. Of three-hole correlations, 44% are also recorded at Site 810. In terms of numbers, 9 potential correlations are recorded between Site 810 and 1 of the 3 transect sites, 4 are 2-hole correlations, and 7 are to 3-hole correlations. There are thus potentially 11 ashes widely distributed over  $4^{\circ}$ – $8^{\circ}$  of latitude and reaching to Shatsky Rise in the northwest Pacific dating from the Miocene. These cover at least 1–2 million  $\text{km}^2$  of seafloor.

If the average thickness of one of these 11 widely distributed ash beds is only 4 cm, its volume over this minimum area of deposition is 40–80  $\text{km}^3$ , erupted approximately once every 270,000 years. This excludes all near-volcano (including subaerial) pyroclastic deposits,

for which no thickness information is available. Moreover, some of the beds are thicker than 4 cm and all are more widely distributed. For the most part, however, thinner ash beds occur in narrower belts, 2°–4° wide, and elongate to the east or southeast. These represent smaller eruptions along a 1200-km arc segment, each of which produced perhaps 5–10 km<sup>3</sup> of dispersed ash every 10,000–15,000 yr. Such volumes are still significantly larger than the 1.1 km<sup>3</sup> of downwind ash estimated for the 18 May 1980 eruption of Mount St. Helens, about half of which fell within 100 km of the volcano (Sarna-Wojcicki et al., 1981).

Almost all *primary* potential correlations to Site 810 in column 1 of Table 1 are to major ash falls (5.7 ± 3.1 cm thick, with a range of 2.0–13 cm) in sites to the west. The 8-cm ash at Shatsky Rise is one of these, but the correlative beds are thinner at two sites to the west. This either has to do with the narrowness of the ash falls (presumably they are thicker *somewhere* to the west), or to the presence of a distal thickness maximum, as described above for the May 1980 Mount St. Helens ash and the Roseau ash of Dominica.

Table 1 also shows a northwesterly predominance of direction of potentially correlative ashes between Shatsky Rise and the sites to the west. There are 6 potential primary correlations to Site 578, leaving 13 to the more northerly Sites 579 and 580 combined. There are 9 secondary potential correlations to Sites 579 and 580, but only 2 to Site 578. This means that most ash plumes and floating pumice came from the North Honshu–Kurile arc system to the west-northwest and northwest if the correlations are valid (Fig. 2).

The glass compositions in Table 2 are sufficiently distinctive to be useful in confirming correlations to Sites 578 through 580. The rhyolites particularly have strongly varying proportions of alkalis (groups 1 and 2 in Fig. 7) and abundances of the minor oxides TiO<sub>2</sub>, MgO, and iron as FeO\*. At this stage we can say that three of four samples analyzed with high-alumina characteristics have primary correlations (as defined in the text) to DSDP Site 578 west of Shatsky Rise, and one to Site 580 to the northwest. The two pumice fragments analyzed both have tholeiitic characteristics; the primary correlations are to Site 578 for the thick pumice mat from Sample 132-810C-6H-6, 18–32 cm, and to Site 580 for the pumice from Sample 132-810C-3H-6, 25 cm. The remaining analyzed ash, Sample 132-810C-4H-1, 4–6 cm, falls in the tholeiitic field in Figure 7, and its primary correlation is to Site 579. The primary correlations are consistent with derivation of tephra from both tholeiitic and high-alumina provinces in Japan and perhaps the Kurile Islands to the west and northwest, but provide no geographical distinction between the two province types. The four primary high-alumina correlations to Site 810 at Sites 578 through 580 average 6.1 cm thick; the three primary tholeiitic correlations average only somewhat less, 4.8 cm thick. These few samples thus suggest little difference in the quantity and explosivity of tephra production from the tholeiitic and high-alumina provinces of Japan.

## DISCUSSION

That pumice and ash should come from the same direction is surprising, since wind directions and currents do not necessarily correspond. However, pumice is also propelled by waves, hence surface winds. Today, Western Pacific frontal systems, originating over Siberia, would tend to push pumice drifting eastward on prevailing currents to the southwest.

Submarine eruptions also produce pumice but little or no ash. These should result in isolated pumice occurrences with no correlations to ash layers. However, large subaerial explosive eruptions in an arc system produce both pumice and ash. To produce floating pumice, the volcanoes have to lie either close to or partly under water. The more pumice an eruption from such a volcano produces, the more likely some of it will survive floating on waves for great distances. Correlations between fairly thick ash beds and more distant pumice

are therefore an indication of very large subaerial eruptions from edifices rising close to or from the ocean.

The 14-cm pumice bed in Hole 810C has potential correlations with a 7-cm ash at Site 578 and a 3-cm ash at Site 579. The latter is definitely fine ash, not pumice. The bed in Hole 810C suggests that a large floating mat of eastward-drifting pumice reached the vicinity of Shatsky Rise, shortly after a major ash fall from the same eruption. The mat dropped quantities of waterlogged pumice as it passed. An idea of how this may have looked is given by Simkin and Fiske (1983), who reprint the description by Capt. Charles Reeves of a very large pumice mat (1170 geographical miles) in the Indian Ocean, through which he guided a ship following the eruption of Krakatau in 1883. Captain Reeves stated that the pumice was concentrated into ridges and that in places “the ocean seemed quite covered with pumice” (Simkin and Fiske, 1983, p. 152). He accurately predicted that the pumice would wash ashore on the east coast of Africa 12 months after the climactic Krakatau eruption.

The arrangement of pumice into “ridges” suggests the action of waves or swells (see also Thorarinsson, 1954, pl. 14B). Waves, particularly, may dash fragile floating pumice fragments against each other. This explains why the pumice dropstones recovered in Hole 810C at Shatsky Rise are rounded, and suggests that they traveled at least part of the way to Shatsky Rise in concentrated pumice mats.

Finally, we can consider the question of whether the near absence of ashes older than 3 Ma at Shatsky Rise is related to climatic factors or to plate motion carrying the rise “within range” of northwest Pacific arcs. The ash stratigraphy at Site 578 extends to 10 Ma, and at Site 579 to 4.27 Ma. At both of these sites, as well as at Shatsky Rise (Table 1), which is some 500 km to the east, the ash frequency increases markedly at about 3 Ma. It also does at Site 436 just east of the floor of the Japan Trench (Fujioka, 1986). The increase in deposition of ash beginning at 3 Ma is thus recorded at all sites seaward of the trench out to distances of 2000 km, on Shatsky Rise.

On the other side of the trench at Site 438, however, extensive ash deposition began about 5 Ma (Fujioka, 1986). Thus the increase in ash deposition at 3 Ma at sites on the Pacific plate does not correspond to a sudden increase in the incidence of explosive volcanism (e.g., Kennett and Thunnell, 1975, 1977; Kennett, 1981). Therefore, climatic controls are strongly indicated. The sudden increase may have resulted either from a sharp increase in jet-stream velocities or from a more expansive seasonal southward migration of the polar-front jet, at about 3 Ma. Similarly, the fairly persistent incidence of pumice at Shatsky Rise since 2 Ma may have resulted from the development of more vigorous winter frontal systems as the continents became glaciated. Western boundary currents also may have begun to circulate more vigorously at about that time.

## SUMMARY AND CONCLUSIONS

Table 1 and Figure 8 present a promising first attempt to establish correlations between air-fall ash and pumice between Hole 810C at Shatsky Rise and sites cored to the west. The potential for ash stratigraphy to provide indications of past wind directions (Eaton, 1963) is borne out by this study. Ash in the northwest Pacific is not simply derived from arc systems to the west, but—at a given location such as Shatsky Rise—from particular sectors of those arc systems that varied through time according to the prevailing conditions of atmospheric circulation. These changed from the Miocene into the Pliocene as climate in northern latitudes became more rigorous. One surprise is that pumice occurrences were as useful in establishing this as ash beds.

The potentially correlative ash beds should provide useful precise stratigraphic markers between Hole 810C, where fairly high biostratigraphic resolution based on nannofossils is possible, to the three sites on the Pacific seafloor to the west. These lie in deep water below the carbonate compensation depth (Heath, Burckle, et al., 1985), and

sediments there are consequently virtually barren of nannofossils and foraminifers.

### ACKNOWLEDGMENTS

This work was supported by a post-cruise award from JOI/US-SAC, here gratefully acknowledged. Prescient reviewers of the post-cruise proposal suggested using Bleil's (1985) high-resolution magnetic stratigraphy at Sites 578 through 580 to provide comparisons with Site 810. I thank Frank Rack and Isabella Premoli Silva for providing the appropriate stratigraphic resolution for Site 810, Julie Dieu for helping to compile the ash logs for Sites 578 through 580, and Genny Healy for getting them into a spreadsheet. Julie Dieu and David Christie provided thoughtful reviews of the manuscript.

### REFERENCES\*

- Berggren, W.A., Kent, D.V., Flynn, J.J., and Van Couvering, J.A., 1985. Cenozoic geochronology. *Geol. Soc. Am. Bull.*, 96:1407–1418.
- Bleil, U., 1985. The magnetostratigraphy of northwest Pacific sediments, Deep Sea Drilling Project Leg 86. In Heath, G.R., Burckle, L.H., et al., *Init. Repts. DSDP*, 86: Washington (U.S. Govt. Printing Office), 441–458.
- Carey, S., and Sigurdsson, H., 1980. The Roseau ash: deep-sea tephra deposits from a major eruption on Dominica, Lesser Antilles arc. *J. Volcanol. Geotherm. Res.*, 7:67–86.
- Conolly, J.R., and Ewing, M., 1970. Ice-rafted detritus in Northwest Pacific deep-sea sediments. In Hays, J.D. (Ed.), *Geological Investigations of the North Pacific*. Mem.—Geol. Soc. Am., 126:219–231.
- Dieu, J.J., 1990. *The Northern Emperors: History of Rejuvenated Alkaline Volcanism and Ice Rafting* [M.Sc. thesis]. Univ. of California, San Diego.
- Eaton, G.P., 1963. Volcanic ash deposits as a guide to atmospheric circulation in the geologic past. *J. Geophys. Res.*, 68: 521–529.
- Fischer, A.G., Heezen, B.C., et al., 1971. *Init. Repts. DSDP*, 6: Washington (U.S. Govt. Printing Office).
- Fujioka, K., 1986. Synthesis of Neogene explosive volcanism of the Tohoku arc, deduced from marine tephra drilled around the Japan Trench region, Deep Sea Drilling Project Legs 56, 57, and 87B. In Kagami, H., Karig, D.E., Coulbourn, W.T., et al., *Init. Repts. DSDP*, 87: Washington (U.S. Govt. Printing Office), 703–726.
- Hays, J.D., and Ninkovich, D., 1970. North Pacific deep-sea ash chronology and age of present Aleutian underthrusting. In Hays, J.D. (Ed.), *Geological Investigations of the North Pacific*. Mem.—Geol. Soc. Am., 126:263–290.
- Heath, G.R., Burckle, L.H., et al., 1985. *Init. Repts. DSDP*, 86: Washington (U.S. Govt. Printing Office).
- Heath, G.R., Rea, D.H., and Levi, S., 1985. Paleomagnetism and accumulation rates of sediments at Sites 576 and 578, Deep Sea Drilling Project Leg 86, western North Pacific. In Heath, G.R., Burckle, L.H., et al., *Init. Repts. DSDP*, 86: Washington (U.S. Govt. Printing Office), 459–502.
- Horn, D.R., Delach, M.N., and Horn, B.M., 1969. Distribution of volcanic ash layers and turbidites in the North Pacific. *Geol. Soc. Am. Bull.*, 80:1715–1723.
- Kennett, J.P., 1981. Marine tephrochronology. In Emiliani, C. (Ed.), *The Sea* (Vol. 7): *The Oceanic Lithosphere*: New York (Wiley), 1373–1436.
- Kennett, J.P., and Thunell, R.C., 1975. Global increase in Quaternary explosive volcanism. *Science*, 187:497–503.
- , 1977. On explosive Cenozoic volcanism and climatic implications. *Science*, 196:1231–1234.
- Krissek, L.A., Morley, J.J., and Lofland, D.K., 1985. The occurrence, abundance, and composition of ice-rafted debris in sediments from Deep Sea Drilling Project Sites 579 and 580, northwest Pacific. In Heath, G.R., Burckle, L.H., et al., *Init. Repts. DSDP*, 86: Washington (U.S. Govt. Printing Office), 647–655.
- Kuno, H., 1965. Fractionation trends of basalt magmas in lava flows. *J. Petrol.*, 6: 302–321.
- Kuno, H., Fisher, R.L., and Nasu, N., 1956. Rock fragments and pebbles dredged near Jimmu Seamount, northwestern Pacific. *Deep-Sea Res. Part A*, 3:126–133.
- Larson, R.L., Moberly, R., et al., 1975. *Init. Repts. DSDP*, 32: Washington (U.S. Govt. Printing Office).
- Nakanishi, M., Tamaki, K., and Kobayashi, K., 1989. Mesozoic magnetic anomaly lineations and seafloor spreading history of the Northwestern Pacific. *J. Geophys. Res.*, 94:15437–15462.
- Natland, J.H., Adamson, A.C., Laverne, C., Melson, W.G., and O'Hearn, T., 1983. A compositionally nearly steady-state magma chamber at the Costa Rica Rift: evidence from basalt glass and mineral data, Deep Sea Drilling Project Sites 501, 504, and 505. In Cann, J.R., Langseth, M.G., Honnorez, J., Von Herzen, R.P., White, S.M., et al., *Init. Repts. DSDP*, 69: Washington (U.S. Govt. Printing Office), 811–858.
- Ninkovich, D., and Donn, W.L., 1976. Explosive Cenozoic volcanism and climatic interpretations. *Science*, 194:899–906.
- Ninkovich, D., Opydyke, N., Heezen, B.C., and Foster, J.H., 1966. Paleomagnetic stratigraphy, rates of deposition, and tephrochronology in North Pacific deep-sea sediments. *Earth Planet. Sci. Lett.*, 1:476–492.
- Ninkovich, D., Shackleton, N.J., Abdel-Monem, A.A., Obradovich, J.D., and Izett, G., 1978. K-Ar age of the late Pleistocene eruption of Toba, North Sumatra. *Nature*, 276:574–577.
- Reiter, E.R., 1963. *Jet-stream Meteorology*: Chicago (Univ. of Chicago Press).
- Rose, W.I., and Chesner, C.A., 1987. Dispersal of ash in the great Toba eruption, 75 ka. *Geology*, 15:913–917.
- Sarna-Wojcicki, A.M., Shipley, S., Waitt, R.B., Jr., Dzurisin, D., and Wood, S.H., 1981. Areal distribution, thickness, mass, volume, and grain size of air-fall ash from the six major eruptions of 1980. *Geol. Surv. Prof. Pap. U.S.*, 1250:577–600.
- Shipboard Scientific Party, 1979. Site 395: 23°N, Mid-Atlantic Ridge. In Melson, W.G., Rabinowitz, P.D., et al., *Init. Repts. DSDP*, 45: Washington (U.S. Govt. Printing Office), 131–264.
- , 1991. Site 810. In Storms, M.A., Natland, J.H., et al., *Proc. ODP, Init. Repts.*, 132: College Station, TX (Ocean Drilling Program), 73–114.
- Simkin, T., and Fiske, R.S., 1983. *Krakatau 1883—the Volcanic Eruption and Its Effects*: Washington (Smithsonian Inst. Press).
- Storms, M.A., and Natland, J.H., 1991. Introduction: seafloor engineering in the Central and Western Pacific. In Storms, M.A., Natland, J.H., et al., *Proc. ODP, Init. Repts.*, 132: College Station, TX (Ocean Drilling Program), 5–22.
- Thorarinsson, S., 1954. The tephra-fall from Hekla on March 29th, 1947. In Einarsson, T., Kjartansson, G., and Thorarinsson, S. (Eds.), *The Eruption of Hekla 1947–1948* (Pt. II): Reykjavik (Visindafelag Islendinga), 1–68.

\* Abbreviations for names of organizations and publications in ODP reference lists follow the style given in *Chemical Abstracts Service Source Index* (published by American Chemical Society).

**Date of initial receipt: 12 August 1992**

**Date of acceptance: 11 June 1993**

**Ms 132SR-301**